The Journal of Chemical Physics

RESEARCH ARTICLE | JULY 01 1992

Photochemical decomposition of AsH_3 on GaAs(100)

X.-Y. Zhu; M. Wolf; J. M. White

J. Chem. Phys. 97, 605–615 (1992)
https://doi.org/10.1063/1.463556

AIP Publishing

Photochemical decomposition of AsH_3 on GaAs(100)

X.-Y. Zhu, M. Wolf, and J. M. White
Department of Chemistry and Biochemistry, Center for Materials Chemistry, University of Texas, Austin, Texas 78712

(Received 22 January 1992; accepted 23 March 1992)

Molecular AsH_3, adsorbed on Ga-rich GaAs(100) at 115 K, dissociates readily upon uv irradiation with 193, 248, and 351 nm excimer laser light. In the initial photodissociation step one As–H bond cleaves, leaving all the AsH_2, and a large fraction of the H, adsorbed to As. The AsH_2 further photodissociates to give As–H and Ga–H. The final steps, photochemical removal of hydrogen from Ga–H and As–H, lead to As deposition. The photodissociation cross section decreases sharply with the extent of photolysis. The wavelength dependence, compared to the gas-phase absorption cross section, extends to much lower photon energies and indicates that substrate-mediated excitation dominates the observed chemistry. There are strong isotope effects in all the cross sections; these are related to mass-dependent substrate-mediated quenching of the excited states. Implications for photon-assisted organometallic chemical vapor deposition are discussed.

I. INTRODUCTION

Organometallic chemical vapor deposition (OMCVD) is one of the most important processes used to manufacture compound semiconductor devices, and laser-assisted OMCVD has potential for the manufacture of next-generation devices. Laser-assisted OMCVD, in principle, can enhance growth rates, lower growth temperatures, promote selective growth, and control growth dimensions with atomic accuracy.[1-8] Obviously, it would be helpful to have a molecular level mechanistic understanding of the surface chemistry involved in these processes. While *gas phase* photochemistry of source molecules may dominate in high-pressure OMCVD, *surface* reactions will dominate in laser-assisted atomic layer epitaxy (ALE) and other low-pressure variants of OMCVD processes. And because the presence of a semiconductor surface introduces new excitation, relaxation, and chemical pathways for the adsorbed molecule,[9,10] knowledge of the gas phase photochemistry of precursors is of limited use. Thus the present study examines the photon-driven surface chemistry of one of the most important precursors to As deposition on GaAs; namely AsH_3.

AsH_3, as well as its alkyl derivatives, are common As source molecules in GaAs OMCVD. During the last few years, there have been persistent efforts to grow GaAs films by photon-assisted OMCVD and ALE using alkyl Ga and AsH_3.[1-8] Given its technological importance, there are surprisingly few studies on the gas phase photochemistry and spectroscopy of AsH_3,[11-15] and even less is known about the surface chemistry of AsH_3. The uv absorption spectrum of gas-phase arsine is continuous below 220 nm but there is some disagreement regarding the existence of a maximum at 184 nm.[11-13] The absorption of a uv photon in this wavelength region promotes AsH_3 to its first excited state, which is dissociative, and gives H and AsH_2 as nascent photoproducts.[11-15] In an attempt to understand the effect of a solid surface on AsH_3 photochemistry, Sasaki *et al.* have recently measured the uv absorbance of AsH_3 condensed on a transparent substrate, silica, and found that it is similar to that of gas-phase AsH_3.[13]

The thermal chemistry of arsine on GaAs(100) has been studied, but not extensively. *Surface*-catalyzed decomposition of AsH_3 is believed to play a dominant role during As deposition in GaAs OMCVD and ALE.[16] Complementing the recent elegant work of Banse and Creighton, using temperature-programmed desorption,[17] we have used high resolution electron energy loss spectroscopy (HREELS), x-ray photoelectron spectroscopy (XPS), and temperature programmed desorption (TPD) to follow the *thermal* decomposition pathway of arsine on both Ga- and As-rich GaAs(100). The details will be published elsewhere,[18] but because of their direct relevance to the present work, we summarize the experimental findings on the Ga-rich GaAs(100) surface: (1) Arsine adsorbs molecularly at 115 K; at saturation, the ratio, based on XPS, of AsH_3 to surface atoms is $\sim$0.16. (2) Upon heating, parent desorption and dissociation, to form AsH_x ($x = 1,2$), set in at temperatures as low as 140 K. (3) Between 200 and 500 K, AsH_x partially recombines with surface hydrogen (AsH_3 desorbs) and partially dissociates irreversibly, leading to As deposition. (4) Near 500 K, molecular H_2 desorbs. While there is no evidence for Ga–H formation associated with the first As–H bond broken, there is good evidence, from HREELS, for its formation during dissociation of AsH_x ($x = 1,2$). Based on XPS, $\sim$15% of the saturation AsH_3 coverage at 115 K irreversibly decomposes to form surface As. A preliminary report of the thermal and photochemistry of arsine on GaAs(100) can be found in Ref. 19.

II. EXPERIMENT

All experiments were conducted in a UHV chamber, pumped by ion, turbomolecular, and Ti sublimation pumps, with a working pressure of 2×10^{-10} Torr. The chamber houses a high resolution electron energy loss spectrometer for vibrational spectroscopy (HREELS), a quadrupole

 0021-9606/92/130605-11$06.00

mass spectrometer for temperature programmed desorption (TPD) and residual gas analysis (RGA), a hemispherical energy analyzer and an x-ray source for x-ray photoelectron spectroscopy (XPS), a low energy electron diffraction (LEED) apparatus, a minibeam ion gun for sputter cleaning, and a 2 μm pinhole collimated molecular doser. The uv light source was a pulsed (11–20 ns) excimer laser (Questec 2110). When filled with different gas mixtures, the laser outputs light at 193 (ArF), 248 (KrF), and 351 nm (XeF). After passing through a series of prisms and apertures, the uv light entered the chamber through a CaF_2 window, uniformly illuminating, along the surface normal, the whole front surface of the sample. To prevent desorption due to thermal heating, the laser pulse energy was kept below 1 mJ/cm^2, unless otherwise noted. This assured that the calculated transient surface temperature rise during irradiation was not more than a few Kelvin (no temperature rise was detected by the thermocouple). The reflected light exited the UHV chamber through the entrance window.

The experiments were done on three rectangular samples ($15\times10\times1$ mm) which were slices of *n*-type GaAs(100) wafers with Si-doping levels ranging from 1×10^{15} to $4\times10^{18}/cm^3$. In terms of AsH_3 photochemistry, these samples were indistinguishable. The sample was held by the edges with two Ta clips which were spot welded to Mo leads. The latter connected to electrically isolated copper blocks which were attached to the manipulator. A 4000 Å thick Ta film was deposited on the sample's backside and served as the predominant electrical pathway for resistive heating. The sample could be cooled by liquid nitrogen to $\sim$115 K and resistively heated to 900 K. The temperature was measured by a chromel–alumel thermocouple spot welded to a small Ta clip which was glued to the bottom edge of the sample with a high-temperature cement (Aremco-571). Cleaning was achieved by Ar ion sputtering, annealing (773 K), and flashing (900 K) cycles. This procedure yields a Ga-rich surface with (4×1) and weak (1×6) LEED features.[20,21]

AsH_3 (99.5%) and AsD_3 (MSD, 98% atom D) were purified by freeze–pump–thaw cycles and dosed through the pinhole doser at 115 K with the doser tube ending about 1 mm from the GaAs surface. This procedure minimizes adsorption on surfaces other than the center portion of the front face ($\sim$60% of the crystal). Reproducible fluxes were obtained by fixing the pressure, measured with a capacitance manometer, of AsH_3 behind the pinhole. *The saturation AsH_3 coverage at 115 K is defined as 1 ML, and corresponds to an adsorbate (AsH_3) concentration of $1\times10^{14}\,cm^{-2}$.*[18]

All HREEL spectra were taken at 115 K with a primary electron energy of 3 eV and a resolution of 60–70 cm^{-1}. Both the incident and detection angles were 60° with respect to the surface normal. To enhance surface sensitivity, XP spectra (Al Kα x-rays; $h\nu = 1435.7$ eV) were taken with a 75° take-off angle. TPD experiments (temperature ramp of 5 K/s) were done with the sample in line of sight and $\sim$6 cm away from the QMS ionizer. The latter was covered by a shroud with a mesh-covered 6 mm ID entrance aperture. This setup, and low ionizer emission current, was employed to reduce electron-stimulated damage of the adsorbates. Over the time required for one experiment, electron-stimulated changes were not detectable.

III. RESULTS

The results will be presented in four parts. Section III A, based on post-irradiation surface analysis (TPD, XPS, and HREELS), is aimed at mapping out the detailed photochemical pathway; Sec. III B describes the photon-fluence dependence and presents results of kinetic modeling; Sec. III C shows the effect of isotope substitution; and the last, Sec. III D compares the photolysis at three wavelengths (193, 248, and 351 nm) and shows the dependence on laser pulse energy. Except for Sec. III D, ArF excimer light (193 nm) was used.

A. Photochemical pathway

TPD. The photodecomposition pathway of AsH_3 adsorbed on Ga-rich GaAs(100)-(4×6) was studied mainly by *post-irradiation* measurements as a function of photon fluence, for example, TPD as detailed in Fig. 1 and summarized in Fig. 2. All TPD areas have been converted to coverages (ML) of As-containing species, relative to the saturation coverage of AsH_3 at 115 K. Only two TPD products, AsH_3 and H_2, were observed in TPD below 820 K. Above 820 K, the sublimation of both Ga and As occur (not shown).[22] The top most spectrum in the left panel of Fig. 1

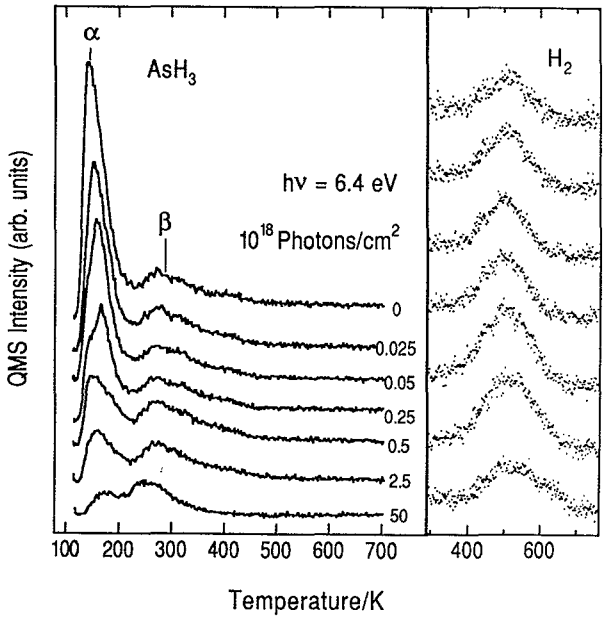

FIG. 1. Left panel: post-irradiation temperature programmed desorption (TPD) spectra of molecular AsH_3 ($m/e = 78$). The GaAs(100)-(4×6) surface was saturated with molecular AsH_3 at 115 K and irradiated with the indicated number of 6.4 eV photons (from top to bottom, 0, 0.025, 0.05, 0.25, 0.5, 2.5, and 50×10^{18} photons/cm^2). The desorption peaks at 144 K and $\sim$300 K are labeled as α and β, respectively. The temperature ramp was 5 K/s. Right panel: temperature programmed desorption (TPD) spectra of H_2 ($m/e = 2$) taken in the same experiments as in the left panel. From top to bottom, the photon fluences are the same as in the left panel.

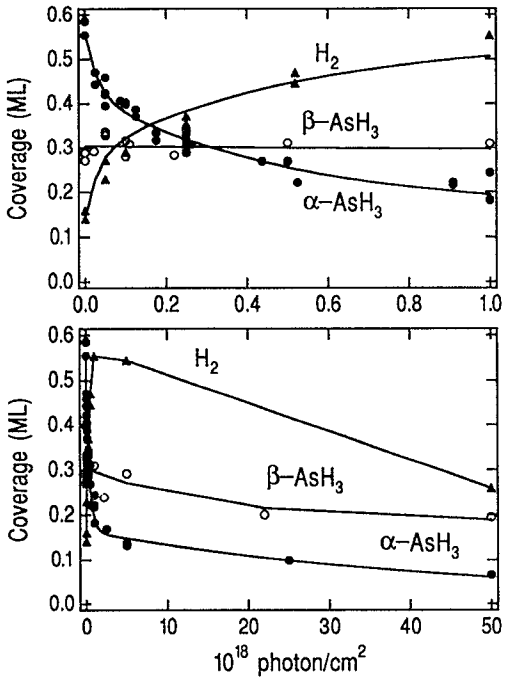

FIG. 2. Post-irradiation TPD areas as a function of photon fluence at 6.4 eV. The data points are obtained from TPD spectra like those in Fig. 1. The solid circles, open circles, and solid triangles are the areas of α-AsH_3, β-AsH_3, and H_2 desorption areas, respectively. The solid lines are fits to kinetic models (see text). There are two fluence scales: (upper) $0–1\times10^{18}$ photons/cm^2 and (lower) panel $0–5\times10^{19}$ photons/cm^2. The AsH_3 coverages are based on the definition that the saturation AsH_3 coverage at 115 K is 1 ML. The H_2 coverage corresponds to As deposition (see text).

shows molecular AsH_3 desorption following a saturation (1 ML) dose at 115 K, but no irradiation. The spectrum is characterized by two desorption peaks, α at 144 K and a broad β peak between 200 and 500 K. The α peak (0.56 ML) corresponds to reversible molecular AsH_3 adsorption and desorption, while β is from the recombination of AsH_x ($x = 1,2$) and surface hydrogen.[18] The α and β peaks probably correspond to different adsorption sites on the Ga-rich GaAs(100) surface; it is well known that the complicated surface reconstructions introduce chemically distinct sites within the unit cell.[20,21] From TPD and quantitative XPS analysis, we find that, of the 1.0 ML saturation AsH_3, 0.44 ML adsorbs on dissociation sites and, during TPD this dissociated arsine follows two routes—0.29 ML recombines to AsH_3 (β-peak) and 0.15 ML irreversibly decomposes to give As deposition and H_2 desorption, shown as the top-most spectrum in the right panel of Fig. 1.[18]

When the arsine-saturated surface was irradiated with 6.4 eV photons (193 nm), three major TPD observations were made (refer to Figs. 1 and 2): (1) With increasing photon fluence (top to bottom in Fig. 1), the area of the α peak decreases. (2) The area of the β peak remains nearly constant, decreasing only when the surface was irradiated with $>5\times10^{19}$ photons/cm^2. (3) The decreasing α-AsH_3 signal is accompanied initially by an increasing H_2 desorption area (right panel of Fig. 1), presumably from the irreversible decomposition of AsH_x ($x = 1,2$) (see below). However, when the fluence is higher than 2.5×10^{18} photons/cm^2, the H_2 TPD area decreases because H is photochemically removed from both Ga–H and As–H species (see below).

The H_2 (or deposited As) coverage (Fig. 2) is calculated, based on the assertion that, during the initial stages of photolysis ($\leqslant1\times10^{18}$ photon/cm^2), the following reaction is operative:

$$\alpha\text{-}AsH_2(a) + h\nu \rightarrow AsH_2(a) + H(g). \quad (1)$$

While more evidence for this assignment will be presented later, it is supported below 1×10^{18} photon/cm^2, Fig. 2, since the decrease in the α-AsH_3 coverage is well accounted for by the increase in H_2 TPD area. The independence of β-AsH_3 desorption peak area on photon fluence indicates a fixed amount (0.15 ML) of thermal deposition of As. This interpretation is supported by the solid lines (calculated, based on the proposed stoichiometry) which nicely fit the experimental data.

With increasing irradiation (lower panel in Fig. 2), the coverage of α-AsH_3 decreases, but much slower, and both β-AsH_3 and H_2 TPD areas decrease. The slow depletion of β-AsH_3 can be modeled by simple first order kinetics with a phenomenological cross section of $\sim5\times10^{-20}$ cm^2. The H_2 TPD area drops, for $>2\times10^{18}$ photon/cm^3, due to photochemical removal of hydrogen from AsH(a) and GaH(a),

$$GaH(\text{or } AsH)(a) + h\nu \rightarrow Ga(\text{or } As) + H(g). \quad (2)$$

We will address this point more clearly later.

HREELS. To establish vibrational character, HREELS data, summarized in Fig. 3, were taken after irradiation of 1 ML of adsorbed arsine with 0, 1.2×10^{18}, 2.5×10^{18}, 1×10^{19}, and 5×10^{19} photons/cm^2. Without irradiation, the HREEL spectrum of 1 ML AsH_3 is characterized by a single loss at 2100 cm^{-1}, corresponding to the H–As stretch of molecular AsH_3.[23] The loss peaks at 287, 574, and 860 are single, double, and triple surface optical phonons, respectively.[24,25] After irradiation with $\leqslant1\times10^{18}$ photons/cm^2, there was no change in the As–H peak position, nor any evidence of the formation of new vibrational features. The latter was unexpected since TPD (Fig. 1) gives an increased amount of H_2 in post-irradiation TPD. However, Eq. (1) provides a simple interpretation, i.e., when the first As–H bond breaks, H desorbs and AsH_2 binds to the surface. In subsequent TPD, H_2 arises when AsH_2 decomposes.

To test this idea, we monitored the photodesorption products during irradiation using the QMS and, indeed, observed only atomic hydrogen in the initial stages. Unfortunately, due to the instability of the QMS at this low mass ($m/e = 1$) and variable background signals, the observation was not consistently reproducible. Following D ($m/e = 2$) from AsD_3 is also difficult because background H_2 interferes. While we conclude that desorption of H occurs, we cannot quantify the portions that desorb and adsorb.

A key finding is that with $>1\times10^{18}$ photons/cm^2, there is a new loss peak at 1860 cm^{-1}, assigned to surface H–Ga.[24,25] With increasing fluence, the Ga–H intensity increases and As–H decreases so that for 5×10^{19} photons/cm^2, surface H–Ga dominates. These observations, along with the TPD results presented in Figs. 1 and 2, sug-

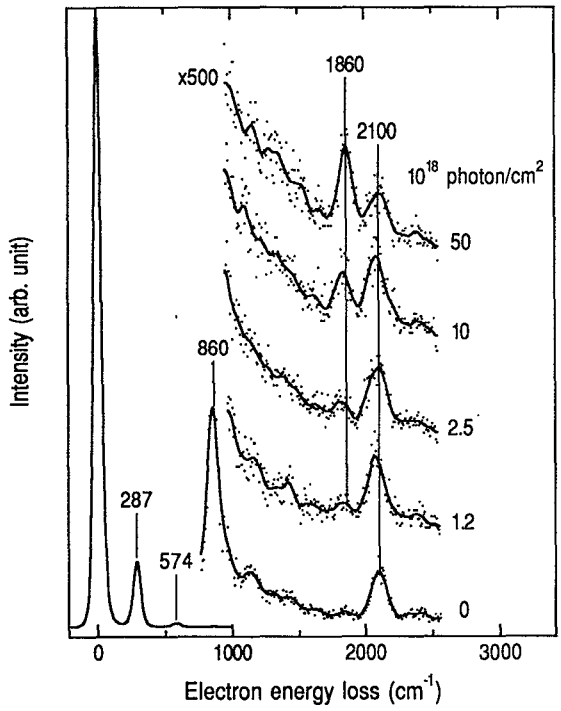

FIG. 3. High resolution electron energy loss spectra taken at 115 K after the AsH_3-saturated GaAs(100)-(4×6) surface was irradiated with the indicated number of 6.4 eV photons at the same temperature. The primary electron energy was 3 eV and the resolution (FWHM) was 60 cm^{-1}. Both the incident and detection angles were 60° with respect to the surface normal. The loss regions are multiplied by a factor of 500. The peaks at 287, 574, and 860 cm^{-1} are the single, double, and triple phonon losses, respectively, while those at 1860 and 2100 cm^{-1} correspond to the H–Ga and H–As stretch vibrations, respectively.

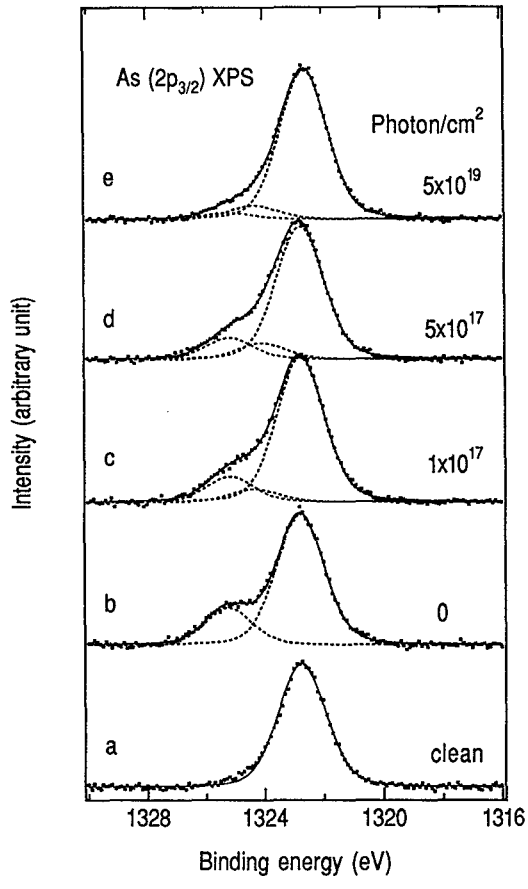

FIG. 4. X-ray photoelectron spectra (As $2p_{3/2}$) taken at 115 K for clean (a) and AsH_3 saturated GaAs(100)-(4×6) surfaces (b)–(e) irradiated with the indicated number of 6.4 eV photons. The spectra were taken with the Al K_α x-rays (1437 eV) and an electron take-off angle of 75°. Each solid line is the sum of deconvoluted fittings (dashed lines) to the data (dots). The background in all the spectra has been removed as described in the text. Spectrum (a) is fit by a single mixed-Gaussian–Lorentzian function (solid line) peaked at 1322.7 eV with a FWHM of 1.9 eV. In addition to this substrate As peak, two new As peaks with higher binding energies, 1325.2 and 1324.3 eV, are deconvoluted from the experimental spectra upon AsH_3 adsorption and irradiation (b)–(e). These two peaks are assigned to surface AsH_3 and AsH_x ($x = 1,2$), respectively.

gest that, while the first step of arsine photodissociation proceeds through the desorption of H and retention of AsH_2 [Eq. (1)], the subsequent photodissociation steps ($> 1\times10^{18}$ photons/cm^2) involve the transfer of hydrogen from As to Ga, i.e.,

$$AsH_2(a) + Ga + h\nu \rightarrow AsH(a) + GaH(a), \quad (3)$$

$$AsH(a) + Ga + h\nu \rightarrow As(a) + GaH(a). \quad (4)$$

XPS. To distinguish molecular and dissociated forms of surface As, we have measured As and Ga core-level XPS at various stages of photolysis. The As ($2p_{3/2}$) and Ga ($2p_{3/2}$) core levels were chosen because they have relatively high binding energies (BE), i.e., low kinetic energies, and are, therefore, surface sensitive. To further enhance surface sensitivity, a photoelectron take-off angle (detection angle with respect to surface normal) of 75° was used. Figure 4 shows a series of As ($2p_{3/2}$) XP spectra for clean (a) and AsH_3 covered (b)–(e) GaAs(100)-(4×6) surface irradiated with the indicated fluences of 6.4 eV photons. In all spectra, the background has been subtracted systematically making use of a linear function augmented by a smoothed step-function fit to the BE regions above and below the peak. For the clean surface (a), the result (dots) can be nicely fit by a single mixed-Gaussian–Lorentzian function (solid line) peaked at 1322.7 eV with a FWHM of 1.9 eV. This XPS peak is from As atoms in the GaAs substrate.

In the presence of other As-containing species, such as AsH_3 and AsH_x ($x = 1,2$), the spectra show additional features on the high BE side of the substrate peak [spectra (b)–(e)]. A least-squares deconvolution routine was used to resolve individual peaks with different binding energies, assuming that all peaks have the same FWHM as the spectrum for clean surface, i.e., 1.9 eV. In spectra (b)–(e), the dashed curves correspond to the deconvoluted peaks while the solid curve is the overall fit to the data. First, for 1 ML AsH_3 and no irradiation, curve (b), the experimental spectrum is nicely fit by two peaks, the substrate As peak at 1322.7 eV and a new As peak at 1325.2 eV. We assign the latter to molecularly adsorbed AsH_3, but we are not able to distinguish α- and β-arsine.

Upon irradiation, the high BE intensity decreases, the low BE intensity increases and there is evidence for an intermediate BE species. This third peak, at an intermediate binding energy, has to be invoked to fit the data, assuming peaks of fixed width and position for the parent arsine and substrate As. We take this as evidence for the presence of photodissociation products, AsH_x ($x = 1,2$). Thus, the post-irradiation spectra were fit with three peaks: (1) 1325.2 eV BE for residual molecular AsH_3, (2) 1322.7 eV BE for substrate As, and (3) an intermediate BE, determined from the fit, for AsH_x ($x = 1,2$). The FWHM of all three was kept constant (1.9 eV) while intensities were taken as fitting parameters. Least-squares fitting to all post-irradiation As ($2p_{3/2}$) XP spectra yields, for AsH_x ($x = 1,2$), an intermediate peak at a binding energy of 1324.3 ± 0.2 eV, i.e., a single intermediate BE characterizes all the spectra. The three deconvoluted peaks are shown as dashed curves in each spectrum. The BE of photochemically deposited As is indistinguishable from that in the GaAs substrate and, with our instrument resolution, AsH and AsH_2 are not resolvable.

As shown in Fig. 4, when the AsH_3 covered surface is irradiated with 1×10^{17} and 5×10^{17} photons/cm^2, the peak for AsH_3 (1325.2 eV) diminishes, the new peak at 1324.3 eV, AsH_x ($x = 1,2$), grows, and the 1322.7 eV peak (substrate As) also grows. At high fluences, such as 5×10^{19}/cm^2 [spectrum (e)], the peak at 1325.2 eV (molecular AsH_3) is nearly gone and the peak at 1324.3 eV also decreases. The latter is the result of photolysis of AsH_x ($x = 1,2$) to As.

The Ga ($2p_{3/2}$) XP spectra (not shown) do not provide much insight into the pathway followed in the photon-driven decomposition of arsine; both the position (1117.1 eV) and FWHM (1.8 eV) remain unchanged upon AsH_3 adsorption and photolysis. In order to reduce data scattering due to experimental uncertainties, we have normalized the As ($2p_{3/2}$) intensities to Ga ($2p_{3/2}$). Figure 5 summarizes these three normalized XPS areas for 1 ML AsH_3 as a function of fluence for 6.4 eV photons. The solid crosses, solid triangles, and open circles describe total As, AsH_3, and AsH_x ($x = 1,2$), respectively (the lines are guides to the eye). Also shown in Fig. 5 is the normalized As signal (thick solid bar) for the clean Ga-rich GaAs(100)-(4×6) surface.

Within experimental error ($\pm 10\%$), the total As($2p_{3/2}$) XPS area remains constant, indicating that *there is negligible desorption of As-containing species during irradiation*. However, significant changes are seen from individual As peaks. For low photon fluences ($\leqslant 1\times10^{18}$ photons/cm^2), the AsH_3 XPS peak area (solid triangles, 1325.2 eV) decreases sharply with fluence, corresponding to the dissociation of AsH_3 and the formation of AsH_x ($x = 1,2$) (open circles, 1324.3 eV). For longer irradiation, more AsH_3 photodissociates, but slowly. Meanwhile, the AsH_x ($x = 1,2$) peak rises quickly, saturates, and then decreases slightly with further irradiation ($> 1\times10^{18}$ photons/cm^2).

Even when Fig. 5 is replotted on a semilogarithmic scale (not shown), the decay of the total AsH_3 coverage with photon fluence remains strongly nonlinear, indicating that simple first order kinetics cannot describe this system. While kinetic details will be presented later, the initial decay of AsH_3 and buildup of AsH_x ($x = 1,2$), gives an initial photolysis cross section of 4×10^{-17} cm^2. Since the measured XPS peak intensity at 1325.2 eV is a sum of contributions from AsH_3 adsorbed in both the α and β states, this cross section is an average. Nevertheless, it agrees with the initial cross section for α–AsH_3 obtained from TPD measurements (see below).

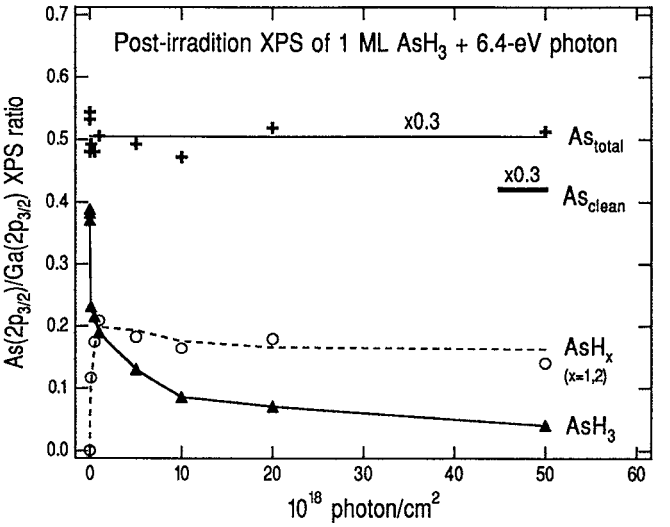

FIG. 5. The areas of As ($2p_{3/2}$) XPS peaks, normalized to that of Ga ($2p_{3/2}$), as a function of photon fluence at 6.4 eV for an AsH_3-saturated GaAs(100)-(4×6) surface at 115 K. The solid crosses are the total As ($2p_{3/2}$) peak areas (×0.3), while the solid triangles and open circles are the areas of individual deconvoluted peaks at 1325.2 and 1324.3 eV (see Fig. 4), respectively. The solid bar is the As ($2p_{3/2}$)/Ga($2p_{3/2}$) ratio (×0.3) for the clean GaAs(100)-(4×6) surface. The lines are guides to the eye.

B. Kinetics and cross sections

We now turn to a quantitative kinetic analysis. Before proceeding, we summarize the pathway. Saturation AsH_3 (1 ML = 1×10^{14} mol/cm^2) adsorbs in at least two ways on Ga-rich GaAs(100). Upon heating, the first gives reversible molecular AsH_3 desorption at 144 K (α-peak, 0.56 ML), while the second dissociates above 140 K and leads to some recombinative desorption between 200 and 500 K (β peak, 0.29 ML) and some As deposition (0.15 ML) and H_2 desorption between 400 and 600 K. The β configuration is relatively photoinactive; significant changes in its TPD intensity are seen only when the arsine-covered surface is irradiated with $\geqslant 5\times10^{19}$ photons/cm^2. Interference from thermal contributions prohibits the use of the β peak as a quantitative measure of the photolysis kinetics. Since the photolysis of α-AsH_3 does not increase recombinative AsH_3 desorption in post-irradiation TPD (β peak in Fig. 1), we believe the two adsorption configurations (α and β) do not communicate, i.e., there is no site exchange or diffusion between the two adsorbed states.

Thus we concentrate on photolysis of the α state. All the evidence suggests that it decomposes in three distinct steps. In the first, one hydrogen is removed to the gas phase and AsH_2 is formed on the surface. In the second step, hydrogen transfers from AsH_2 to surface Ga. In the third step, hydro-

gen is photochemically desorbed from both GaH and AsH. All the photodissociation products, AsH_x ($x = 1,2$) and GaH, lead to H_2 desorption in post-irradiation TPD. An alternative, photon-driven removal of two hydrogens from $AsH_3(a)$ and the direct formation of $AsH(a)$, is unlikely because: (1) the mass balance, based on Eq. (1), for α-AsH_3 depletion and H_2 formation in TPD (upper panel of Fig. 2) is satisfactory, and (2) atomic, not molecular, hydrogen desorption is observed during irradiation.

In the following, we analyze the kinetics and obtain a cross section for each step based on post-irradiation TPD, as well as HREELS measurements. All cross sections are referenced to the *incident* photon fluence. To avoid explicit assumptions about the excitation mechanism, no account has been taken of light absorption in and reflection from the substrate.

The kinetics of the first step can be obtained from post-irradiation AsH_3 TPD areas of the α state (144 K peak). This is shown on a semilogarithmic scale in Fig. 6 for two fluence ranges. Over the whole fluence range [lower panel ($0–5\times10^{19}$ photons/cm^2)], the molecular AsH_3 coverage does not drop linearly with photon fluence. However, at photon fluences $>2\times10^{18}$/cm^2 (lower panel) there is clearly a linear region with a cross section of $\sim10^{-20}$ cm^2 for the remaining AsH_3 ($\sim$0.16 ML), while for photon fluences $<2\times10^{18}$/cm^2, the *effective* cross section is much higher ($>1\times10^{-18}$ cm^2). It is natural to postulate from this observation that, within the α-molecular state, arsine adsorbs on at least two kinds of adsorption sites with distinctively different photolysis cross sections.

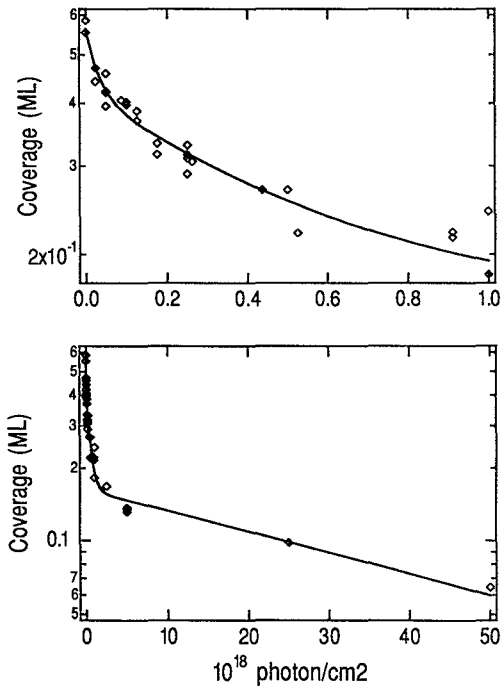

FIG. 6. The surface coverage (open diamonds) of α-AsH_3 as a function of photon fluence at 6.4 eV (193 nm). The data points are obtained from post-irradiation TPD spectra like those in Fig. 1. The solid line is from the kinetic model assuming three nonequivalent sites for α-AsH_3 [Eq. (5), see text]. The figure is presented on two scales: $0–1\times10^{18}$ photons/cm^2 in the upper panel and $0–5\times10^{19}$ photons/cm^2 in the lower panel.

Turning to short irradiations ($0–1\times10^{18}$ photons/cm^2), we found that, even during the initial stages of photolysis, the logarithm of coverage does not drop linearly with photon fluence (upper panel of Fig. 6). If all arsine adsorption sites were equivalent, we would expect the cross section to change only when substantial amounts of photochemical products have accumulated on the surface, enough to affect either the excitation or the relaxation channels. This assumption obviously contradicts the results presented in the upper panel. *Therefore, the data cannot be explained by simple first order kinetics involving one type of adsorbed α-AsH_3.*

We now consider a more detailed model which is consistent with all our observations. Given the knowledge that the complicated dimerization on clean Ga-rich GaAs(100)-(4×6) results in multiple possible sites for AsH_3 adsorption,[20,21] we postulate that the α arsine state actually involves three adsorption sites with distinctly different photolysis cross sections. At least three are required to satisfactorily fit the experimental data. In this regard recall that, in a recent careful TPD study, Banse and Creighton found that the α-desorption peak in TPD (Fig. 1) is a sum of at least two peaks.[17] The data (Fig. 6) could not be fit assuming only two adsorption sites because of the curvature found at low fluence. Our proposed three-state model gives the following kinetic equation for the surface coverage (θ) of α-AsH_3:

$$\theta_{AsH_3} = \theta_1 \exp(-\sigma_1 N_{ph}) + \theta_2 \exp(-\sigma_2 N_{ph}) + \theta_3 \exp(-\sigma_3 N_{ph}), \quad (5)$$

where N_{ph} is the photon fluence, and θ_1, θ_2, and θ_3 are the saturation coverages of AsH_3 on the three postulated sites.

We have fit the data with this model, using a least-square fitting routine. The result is shown as the solid curve (upper and lower panels of Fig. 6) which agrees very satisfactorily with the experimental data for the whole fluence region. The calculated coverages of the three sites are: 0.14 ± 0.1, 0.26 ± 0.1, and 0.16 ± 0.1 ML, respectively. The corresponding cross sections are $\sigma_1 = 3.6\pm0.5$ ($\times10^{-17}$), $\sigma_2 = 1.9\pm0.3$ ($\times10^{-18}$), and $\sigma_3 = 2.0\pm0.3$ ($\times10^{-20}$) cm^2. The error bars are obtained from independent fits to different sets of experimental data. With different initial estimates, the fitting always converges to the results presented above.

The cross section of the second photodissociation step, i.e., the transfer of hydrogen from $AsH_2(a)$ to surface Ga, can be estimated from the HREELS data presented in Fig. 3. From the growth of the Ga–H stretch loss peak at 1860 cm^{-1}, we estimated a cross section of $3\pm1\times10^{-20}$ cm^2 for the photodissociation of AsH_2.

The cross section for the last photolysis step, i.e., the removal of hydrogen from both AsH and GaH, is obtained from post-irradiation TPD measurements. The AsH and GaH covered surface was prepared by annealing an arsine-saturated surface at 400 K.[18,19] The H_2 TPD area was used as a measure of surface hydrogen coverage as a function of

subsequent photon fluence at 6.4 eV. The data is shown as open triangles on a semilogarithmic scale in Fig. 7. From the slope of the least-squares linear fit, we obtained a cross section of 1.6×10^{-21} cm^2. The solid circles in Fig. 7 will be discussed in the next paragraph.

C. Isotope effects

During a *surface* photochemical event, the presence of *substrate* electronic states introduces efficient relaxation channels for the excited adsorbate. As a result, the probability of a photolysis process will depend strongly on the lifetime of the adsorbate on the excited state potential energy surface (PES). Since a lighter particle is accelerated in a shorter time on the excited PES, strong isotope effects can be expected in the cross sections of surface photoreactions and can provide insight into the dynamics.[26-29] For this purpose, we have measured the cross sections of the initial and final photochemical steps for AsD_3 adsorbed GaAs(100).

For the final stages, Fig. 7 shows (solid circles), in semilogarithmic form, the deuterium coverage (on both Ga and As sites) as a function of photon fluence at 6.4 eV. A linear least squares fit (solid circles) gives a photolysis cross section of 1.2×10^{-21} cm^2. This gives an isotope effect (σ_H/σ_D) of 1.3 ± 0.1 for the last step of arsine photolysis on GaAs(100)-(4×6).

Similarly, we have also measured the isotope effect in the early stages, the removal of one hydrogen from adsorbed arsine. This is shown in Fig. 8 for the α-state molecular arsine coverage as a function of photon fluence at 6.4 eV (solid circles for AsD_3 and open triangles for AsH_3). The solid lines are fits to the kinetic model presented above. In the fitting, the coverages of the sites are kept constant as determined from Fig. 6, while cross sections are allowed to vary. For AsD_3 (solid circles), we found $\sigma_1 = 1.9\times10^{-17}$ and $\sigma_2 = 9.3\times10^{-19}$ cm^{-2}. Fitting to the open triangles (reproduced from Fig. 6) gives, for AsH_3, $\sigma_1 = 3.6\times10^{-17}$, $\sigma_2 = 1.9\pm0.3\times10^{-18}$ cm^{-2}. Therefore, the isotope effect for ($\sigma_{AsH_3}/\sigma_{AsD_3}$) is 1.9 for σ_1 and 2.0 for σ_2. Within experimental error, these two numbers are identical. Interestingly, if we divide the fluence scale (x axis) for AsD_3 by a factor of 1.9 ± 0.2, all the data (D and H) lie on the same curve. This gives, independently, an isotope effect of 1.9 ± 0.2 for the first step ($0-1\times10^{18}$ photons/cm^2).

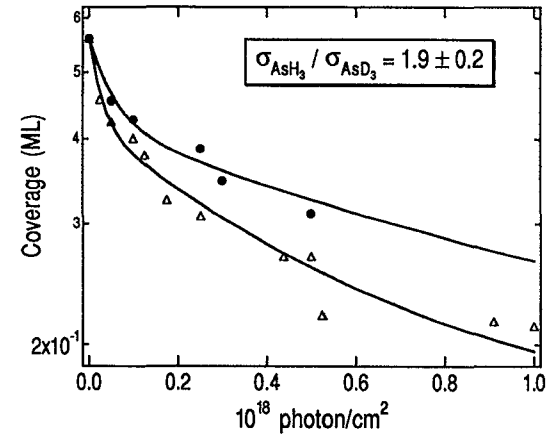

FIG. 8. The surface coverage of α-AsH_3 (open triangles) and α-AsD_3 (solid circles) as a function of photon fluence at 6.4 eV (193 nm). The AsH_3 data is reproduced from Fig. 6 while the AsD_3 data was taken under the same conditions as in Fig. 6. The solid lines are from the kinetic model presented in Fig. 6 [Eq. (4), see text]. The fitting yields a constant isotope ratio ($\sigma_{AsH_3}/\sigma_{AsD_3}$) of 1.9 ± 0.2 for the depletion of α-state molecular arsine.

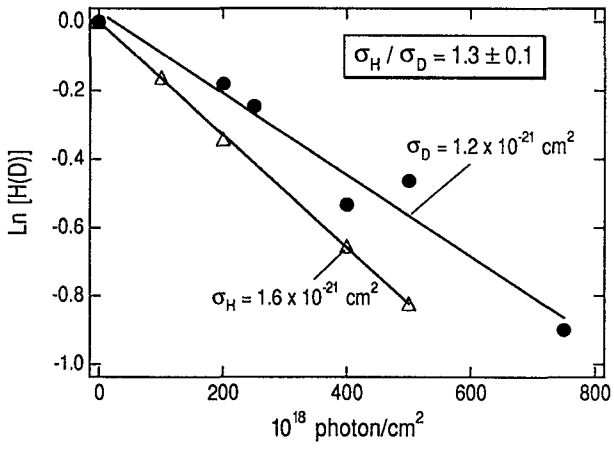

FIG. 7. The logarithm of post-irradiation TPD areas of H_2 (open triangles) and D_2 (solid circles) as a function of photon fluence at 6.4 eV (193 nm). The hydrogen or deuterium covered surface was prepared by flashing an arsine saturated GaAs(100)-(4×6) surface (115 K) to 400 K. The data points are obtained from TPD spectra taken after the surface was irradiated with 6.4 eV (193 nm) photons. The laser pulse energy used in this experiment was 4 mJ/cm^2. The solid lines are least-squares linear fits to the experimental data. The slope of the fits give photodesorption cross sections of 1.6×10^{-21} and 1.2×10^{-21} cm^2 for surface hydrogen and deuterium, respectively. The isotope ratio for this process is (1.3 ± 0.1).

D. Dependence on wavelength and pulse energy

The results presented above were obtained with 193 nm (6.4 eV) light. We have also measured the wavelength dependence. The upper panel in Fig. 9 shows, in the low fluence region ($0-2.5\times10^{18}$ photons/cm^2), the post-irradiation α-AsH_3 TPD area as a function of photon fluence at three wavelengths (193 nm, solid squares; 248 nm, open triangles; and 351 nm, crosses). Clearly, the photolysis cross section decreases with increasing wavelength, but this data can be put on a single "universal" curve as follows. Using Eq. (5) and coverages used to fit Fig. 6, all the cross sections (σ_{1-3}) determined from Fig. 6 are divided by a constant, C, which is taken as the only variable in fitting the wavelength dependence. This yields $C = 1.0$ for 193 nm, 2.3 for 248 nm, and 7.7 for 351 nm. This assumption implies that the three cross sections (σ_{1-3}) have the same wavelength dependence and, as demonstrated in the lower panel of Fig. 9, gives a very good fit over the whole fluence region ($0-5\times10^{19}$ photons/cm^2) studied. Therefore, going from 193 nm to 248 and 351 nm, the cross sections decrease by a factor of 2.3 and 7.7, respectively.

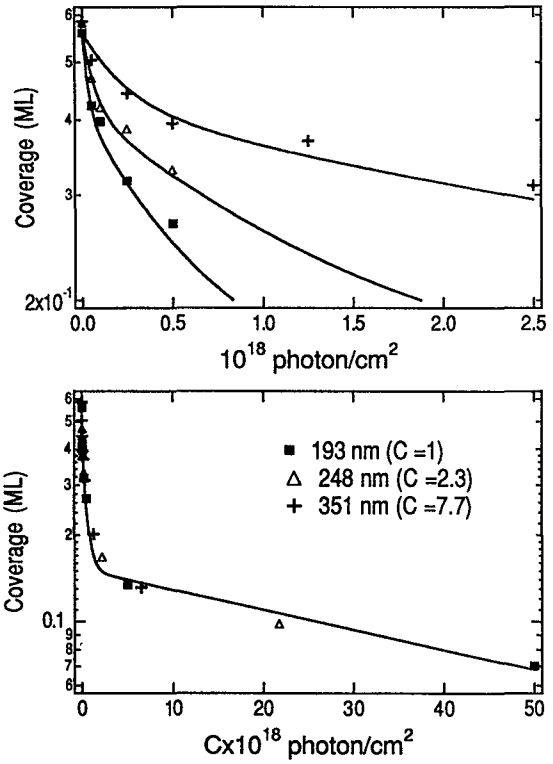

FIG. 9. Upper panel: the surface coverage of α-AsH_3 as a function of photon fluence (0–2.5$\times 10^{18}$ photons/cm^2) at 193 nm (solid squares), 248 nm (open triangles), and 351 nm (crosses), respectively. The data points are obtained from post-irradiation TPD spectra like those in Fig. 1. The solid lines are from kinetic models like that in Fig. 6. See text for details. Lower panel: the same data as in the upper panel, but presented for larger photon fluence range with a variable x axis. Please note the different x scales for 193, 248, and 351 nm light. The solid line, reproduced from the kinetic fit in Fig. 6, is on the same x-scale as the data at 193 nm.

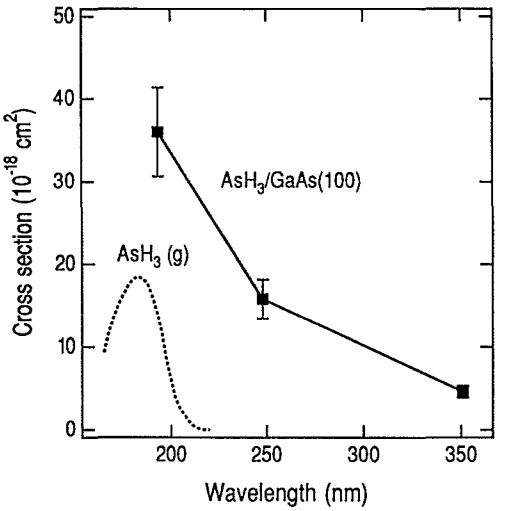

FIG. 10. The initial photodissociaton cross section (σ_1, solid squares) as a function of light wavelength for α-state molecular AsH_3 adsorbed on the GaAs(100)–(4×6) surface. The dashed curve is the uv absorption spectrum for gas phase AsH_3, reproduced from Ref. 13 (after Sasaki *et al.*, 1989).

Turning to a comparison with gas phase arsine, Fig. 10 plots the gas phase arsine uv-adsorption spectrum, dashed curve, reproduced from Ref. 13 and the initial adsorbed arsine photodissociation cross section, taken to be σ_1. In the gas phase, the absorbance is negligible at wavelengths above 220 nm. However, the surface photolysis of arsine extends to wavelengths longer than 351 nm, pointing to an excitation mechanism involving the substrate, probably photon-driven charge transfer from the substrate to the adsorbate.

While most of the data presented above were obtained with laser pulse energies below 1 mJ/cm^2, the dependence of photolysis yield on the laser pulse energy was studied at all three wavelengths. Using pulse energies between 0.3 and 8 mJ/cm^2, while keeping the photon fluence constant, we found the yield (not shown), based on TPD, was independent of pulse energy. This implies that the photo yield per pulse increases linearly with pulse energy between 0.3 and 8 mJ/cm^2, clearly implicating contributions from a nonthermal mechanism.

IV. DISCUSSION

A. Adsorption

The above results demonstrate that the thermal and photo chemistry of arsine on GaAs(100) is state or site dependent, although the precise nature of these sites remains, for the most part, unknown. In the following, we present plausible interpretations based on reported structural models.

On semiconductors, many surface atoms are not fully coordinated and the localized valence electrons in these unsaturated atoms are usually called dangling bonds. These have high free energy and often the surfaces reconstruct to lower the free energy, e.g., they may dimerize to form dimer bonds. Because of their lability, adsorption, and chemical reaction at dangling bond surface sites is often invoked, sometimes involving the breaking and remaking of dimer bonds. The local atomic structure around these unsaturated atoms and, thus, the reactivity and electronic properties of these dangling bonds, often varies within the surface unit cell, i.e., there are distinct sites. The site selectivity of semiconductor surface chemistry is demonstrated by recent studies on well-characterized Si surfaces.[30] For example, on Si(111)–(7×7), the reaction of Si_2H_6 occurs preferentially at the so-called rest-atom sites,[30(c)] while the early stage of Si oxidation involves preferentially the faulted-half of the 7×7 unit cell and corner adatom sites.[30(b)] Site specificity has also been observed in photoassisted oxidation of Si(111)[31] and in laser-induced desorption of NO from Si(111).[32]

Compared to Si, the GaAs(100) surface is not as well understood. The Ga-rich GaAs(100)–(4×6) surface used in this study is composed of (4×1) and (2×6) domains.[20] The "4×1" domain is actually a $c(8\times2)$ reconstruction. Based on scanning–tunneling microscopy images, Biegelsen *et al.* recently proposed structural models for various reconstructions of GaAs(100).[21] Figure 11 shows the proposed ball-and-stick models for the Ga-rich (2×6) and $c(8\times2)$ reconstructions. For the $c(8\times2)$ reconstruction, which has no surface bonded As, the (4×2) subunit within the

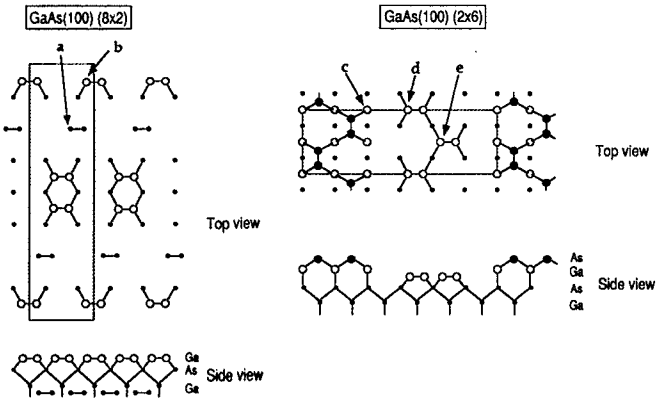

FIG. 11. Possible ball-and-stick models for the $c(8\times2)$ and (2×6) domains on the GaAs(100)-(4×6) surface (after Biegelsen *et al.*, 1990, Ref. 21). The arrows indicate likely adsorption sites for molecular arsine.

$c(8\times2)$ unit consists of two dimers adjacent to one another and two missing dimers. The (2×6) reconstruction, on the other hand, has both As and Ga dimers in its surface. The coexistence of domains of "4×1" and 2×6 has been observed in STM for the Ga-rich GaAs(100) surface with (4×6) LEED symmetry.[21] These structural models, while not necessarily unique, are consistent with what is known.

Using these structural models, we now discuss plausible sites for arsine adsorption and dissociation. Intuitively, we expect the adsorption of AsH_3 on a Ga-rich surface to involve the formation of a donor–acceptor bond between AsH_3 (donor) and surface Ga (acceptor). We can identify at least five possible Ga sites within the structure of Fig. 11 [labeled (a),(b),...,(e)]. We believe the β state involved in *thermal dissociation* probably involves adsorption sites like (c) and (a) because there are neighboring As sites; XPS results indicate that AsH_3 adsorbed on the Ga-rich GaAs(100) thermally dissociates below 200 K but H–Ga species are seen in HREELS only when the arsine covered surface is heated to above 200 K.[18] Therefore, thermal dissociation probably transfers H to As. The photochemically active α molecular adsorption state may involve sites such as (b), (d), and (e). The difference in the electronic properties may result in different excitation probabilities for molecular arsine adsorbed on these sites. This may well be the reason for the observed kinetics in Sec. III B.

B. Excitation and relaxation

Photochemistry on semiconductor surfaces has been studied for a number of adsorbates.[31–37] While direct electronic excitation of the adsorbate has been found for a few systems, such as $Mn(CO)_6$ on Si,[34] most of the experimental evidence suggests the dominance of substrate mediated excitation processes.[30–33,35–37] These usually involve the attachment of photoexcited substrate carriers (electrons and holes) to the adsorbate or photoassisted charge transfer from surface states to the adsorbate.

For arsine photodissociation on GaAs(100), the evidence, including the negligible calculated surface temperature jump, the linear pulse-energy dependence, and the wavelength dependence in Fig. 10, rules out the involvement of thermal heating in the observed photochemistry. Direct electronic excitation of adsorbed arsine can also be ruled out by the observed wavelength dependence. As shown in Fig. 10, the onset of AsH_3 photolysis on GaAs(100) is >351 nm (<3.5 eV) while that for the gas-phase absorbance is <220 nm (>5.7 eV). Since α-state AsH_3 is weakly held on the surface, it is not sensible that the spacing between excited and ground state energy levels within AsH_3 can be perturbed by more than 2.2 eV upon adsorption. We conclude that the excitation mechanism involves the substrate, at least at wavelengths longer than the gas phase absorption threshold. While direct photoexcitation of adsorbed arsine is plausible at 193 nm, the common kinetics observed at all wavelengths (lower panel of Fig. 9) argues against this possibility.

Considering substrate excitation, two possibilities must be considered: (1) dissociative attachment of photoexcited bulk substrate carriers, most probably hot electrons, to the adsorbate or (2) photoassisted charge transfer from surface states to the adsorbate. While these two mechanisms are not easily distinguishable, we favor the latter because of the continually changing cross section (Fig. 6). If there are a variety of surface sites (minimum of three according to our fits) then the results can be understood. On the other hand, it is difficult to see how a slight change in the surface concentrations would affect the hot-carrier yield significantly.

In this context, it is important to note that the decreasing cross section with the extent of photolysis is not a result of increasing quenching efficiency because the constant isotope effect in Fig. 8 indicates a constant quenching probability (see below). Therefore, the change in photolysis rate has to be attributed to excitation. The kinetic modeling (Sec. III B) suggests that α-state arsine involves at least three different surface sites with distinctively different cross sections. This is consistent with the proposed excitation mechanism involving charge transfer from surface states to the adsorbate. Although the binding energies of arsine on these postulated sites may be too small to be distinguishable in TPD, the difference in the electronic properties of these sites, e.g., electron occupancy and energy level, is certainly expected to influence the probability of photoassisted charge-transfer excitation. Similar site-specific photoassisted charge-transfer excitation processes have been reported for the laser-induced desorption of NO on Si(111)[32] and photoassisted oxidation of Si(111).[31]

Having discussed the excitation mechanism, we now turn to an analysis of the excitation cross sections and relaxation probabilities. As set forth in Sec. III C, the presence of efficient quenching by the substrate leads to strong isotope effects. Similar effects have been observed in electron-stimulated desorption (ESD) studies[26,28] and have been taken as evidence for the Menzel–Gomer–Redhead (MGR) model.[27] Recently, isotope effects have been observed in surface photochemical reactions.[29]

Assuming a surface photoreaction (dissociation or desorption) with an experimental cross section, σ, which is a product of the excitation cross section, σ_e, and the total probability of dissociation/desorption, P,

$$\sigma = \sigma_e P. \quad (6)$$

Since the uv absorption spectra of gas-phase arsine shows negligible isotope shifts,[11-13] and considering the broadening expected for electronic energy levels on the surface, we believe the electronic energy levels of adsorbed AsH_3 and AsD_3 are essentially identical. Therefore, we can safely assume that the excitation cross section, σ_e, is independent of isotope substitution.

The MGR model for electronic transitions on surfaces assumes a critical distance, z_c, for bond stretching on the excited state PES.[10,27-29] Deexcitation at $z < z_c$ results in quenching of the excited state, while at $z > z_c$, the particle has gained enough kinetic energy to overcome the barrier for recapture on the ground state PES and, thus, bonds break. With this assumption, it can be shown[27-29] that, for two isotopically-labeled species with masses m_1 and m_2, the isotope effect is given by

$$\sigma_{m_1}/\sigma_{m_2} = (1/P_{m_1})^{(m_2/m_1)^{1/2}-1}. \quad (7)$$

For the photochemical removal of hydrogen (deuterium) from As or Ga, $m_2/m_1 = 2$. From Eq. (6) and the results in Fig. 7, we calculate, for the photodesorption of hydrogen from AsH and GaH, an excitation cross section of 3.2×10^{-21} cm^2, and, once excited, a desorption probability of 0.5. Similarly, for the photodissociation AsH_3 to AsH_2, we calculate, from Fig. 8, a dissociation probability of 0.2. The excitation cross sections are 1.8×10^{-16} cm^2 and 9.5×10^{-18} cm^2 for sites 1 and 2, respectively. These parameters are summarized in Table I.

C. Implications for OMCVD and ALE of GaAs

GaAs-based compound semiconductors are often called "materials for the future,"[38] and one future will be aided by the development of low-temperature growth processes under kinetically controlled conditions. This development, differing from conventional OMCVD processes where mass-transport is the rate-limiting step, will be dominated by surface reaction control. Since a lower substrate temperature results in a slower rate for surface reactions, in most cases, reasonable epitaxial growth rate can be realized only with nonthermal activation, e.g., uv photon irradiation. Recently, there have been several studies involving uv-assisted growth of GaAs films.[1-8] While enhanced growth at low temperatures is observed in all cases, the actual mechanisms are not known. The present study sheds light on the mechanism of uv-assisted As deposition, particularly at low pressures where surface reactions dominate.

Our study indicates that, while the low overall cross section ($\sim10^{-21}$ cm^2 at 193 nm) for the total removal of hydrogen from GaAs(100) probably makes photochemical As deposition impractical, the high initial uv photodissociation cross section ($\sim4\times10^{-17}$ cm^2 at 193 nm) is a reasonable way to enhance the first step. This is significant since the first step is often rate limiting. From a practical perspective, it is well known that lowering the AsH_3 pressure during GaAs growth is limited by its low reactive sticking coefficient, on the order of 10^{-6}.[22] Thus, most molecular arsine, transiently trapped on the surface (precursor to dissociation), desorbs back to the gas phase under growth conditions, and only a very small portion overcomes the dissociation barrier and eventually leads to As deposition. However, under uv irradiation, the ratio of dissociation to desorption for precursor arsine can be significantly increased. In this connection, it is important to note that gas-phase uv enhancement operates only at wavelengths shorter than 220 nm while surface uv enhancement, since it involves the substrate, can be extended to wavelengths longer than 351 nm (Fig. 10).

V. SUMMARY

The results presented above can be summarized as follows:

(1) Molecular arsine, adsorbed on the Ga-rich GaAs(100)-(4×6) surface at 115 K, dissociates upon uv irradiation between 193 and 351 nm, a result of substrate-mediated excitation probably involving charge transfer from surface states to the adsorbate. The initial photolysis cross section decreases with the increase in wavelength.

(2) The photodissociation of adsorbed AsH_3 proceeds step-wise, leading to the sequential formation of AsH_2, AsH, GaH, and, finally, to As deposition. There is no evidence of removal of As containing species during irradiation.

(3) The photochemical cross section decreases with the extent of photolysis. At 193 nm, the initial cross section for the first photodissociation step [$AsH_3(a) \rightarrow AsH_2(a) + H(g)$] is 4×10^{-17} cm^2, while that for the last step [GaH or AsH → Ga or As + $H(g)$] is 1.6×10^{-21} cm^2.

TABLE I. Cross sections for individual photolysis steps.

Photodissociation step		Excitation cross section(cm^2) 193 nm	Photolysis cross section (cm^2) 193 nm	248 nm	351 nm
$AsH_3(a) \rightarrow AsH_2(a) + H(g)$	(initial)[a]	$\sim1.8\times10^{-16}$	$3.6\pm0.5\times10^{-17}$	$1.6\pm0.2\times10^{-17}$	$4.7\pm0.7\times10^{-18}$
	(final)[a]		$2.0\pm0.3\times10^{-20}$	$8.7\pm0.9\times10^{-21}$	$2.6\pm0.4\times10^{-21}$
$AsH_2(a) \rightarrow AsH(a) + GaH(a)$			$\sim3\pm1\times10^{-20}$		
GaH or $AsH(a) \rightarrow H(g)$		$\sim3.2\times10^{-21}$	$1.6\pm0.1\times10^{-21}$		

[a] The initial and final cross sections for this step are approximated by σ_1 and σ_3, respectively, in the kinetic modeling (see text).

(4) Isotope effects (D for H) are observed in the cross sections for all photodissociation steps and have been attributed to substantial quenching of the excited states by the substrate: for the first step of photolysis, 80% of all excited adsorbates are quenched while for the last step, 50% are quenched.

(5) This study indicates that, for GaAs OMCVD at low substrate temperatures and low arsine pressures, photon excitation of the surface can increase the rate of As deposition by enhancing the *effective* initial dissociative sticking coefficient of AsH_3.

ACKNOWLEDGMENTS

We thank Professor R. Dupuis and M. Arendt for their help with the GaAs wafer, and Dr. B. Banse and Dr. J. R. Creighton for many discussions and for generously providing the AsD_3 sample. M. W. acknowledges a Feodor–Lynen research fellowship of the Alexander-von-Humboldt Society. This work was supported in part by the Science and Technology Center Program of the National Science Foundation, Grant No. CHE 8920120.

[1]A. Usuri and H. Watanabe, Ann. Rev. Mater. Sci. **21**, 185 (1991).
[2]A. Doi, Y. Aoyagi, and S. Namba, Appl. Phys. Lett. **49**, 785 (1986).
[3]N. Putz, H. Heinecke, E. Veuhoff, G. Arens, M. Heyen, H. Luth, and B. Balk, J. Cryst. Growth **68**, 194 (1984).
[4]P. Balk, M. Fisher, D. Grundmann, R. Luckerath, H. Luth, and W. Richter, J. Vac. Sci. Technol. B **5**, 1453 (1987).
[5]V. M. Donnelly, V. R. McCrary, A. Applebaum, D. Brasen, and W. P. Lowe, J. Appl. Phys. **61**, 1410 (1987).
[6]S. S. Chu, T. L. Chu, C. L. Chang, and H. Firouzi, Appl. Phys. Lett. **52**, 1243 (1988).
[7]J. Nishizawa, T. Kurabayashi, H. Abe, and N. Sakurai, J. Vac. Sci. Technol. A **5**, 1572 (1987).
[8]H. Liu, J. C. Roberts, J. Ramdani, S. M. Bedair, J. Farari, J. P. Vilcot, and D. Decoster, Appl. Phys. Lett. **58**, 388 (1991).
[9]W. Ho, Comments Cond. Mat. Phys. **13**, 293 (1988).
[10]X.-L. Zhou, X.-Y. Zhu, and J. M. White, Surf. Sci. Rep. **13**, 73 (1991).
[11]C. M. Humphries, A. D. Walsh, and P. A. Warsop, Discuss. Faraday Soc. **35**, 148 (1963).
[12]R. F. Karlicek, B. Hammarlund, and J. Ginocchio, J. Appl. Phys. **60**, 795 (1986).
[13](a) M. Sasaki, Y. Kawakyu, and M. Mashita, Japanese J. Appl. Phys. **28**, L131 (1989); (b) M. Sasaki, Y. Kawakyu, H. Ishikawa, and M. Mashita, Appl. Surf. Sci. **41**, 342 (1989).
[14]T. Ni, Q. Lu, X. Ma, S. Yu, and F. Kong, Chem. Phys. Lett. **126**, 417 (1986).
[15]B. Koplitz, Z. Xu, and C. Wittig, Appl. Phys. Lett. **52**, 860 (1988).
[16]F. T. J. Smith, Prog. Solid State Chem. **55**, 111 (1989).
[17]B. A. Banse and J. R. Creighton, Surf. Sci. (in press).
[18]M. Wolf, X.-Y. Zhu, T. Huett, and J. M. White, Surf. Sci. (in press).
[19]X.-Y. Zhu, M. Wolf, T. Huett, J. Nail, B. A. Banse, J. R. Creighton, and J. M. White, Appl. Phys. Lett **60**, 977 (1992).
[20](a) P. Drathen, W. Ranke, and K. Jacobi, Surf. Sci. **77**, L162 (1978); (b) M. D. Pashley, K. W. Haberern, W. Friday, J. M. Woodall, and P. D. Kirchner, Phys. Rev. Lett. **60**, 2176 (1988).
[21]D. K. Beigelsen, R. D. Bringans, J. E. Northrup, and L.-E. Swartz, Phys. Rev. B **41**, 5701 (1990).
[22]J. R. Creighton and B. A. Banse, Mater. Res. Soc. Symp. Proc. **222**, 15 (1991).
[23]V. M. McConagie and H. H. Nielsen, Phys. Rev. **75**, 633 (1949).
[24]H. Luth and R. Matz, Phys. Rev. Lett. **46**, 1652 (1981).
[25]L. H. Dubois and G. P. Schwartz, Phys. Rev. B **26**, 794 (1982).
[26]T. E. Madey, J. T. Yates, Jr., D. A. King, and C. J. Uhlander, J. Chem. Phys. **52**, 5215 (1970).
[27](a) D. Menzel and R. Gomer, J. Chem. Phys. **41**, 3311 (1964); (b) P. A. Redhead, Can. J. Phys. **42**, 886 (1964).
[28]R. D. Ramsier and J. T. Yates, Jr., Surf. Sci. Rep. **12**, 243 (1991).
[29]M. Wolf, S. Nettesheim, J. M. White, E. Hasselbrink, and G. Ertl, J. Chem. Phys. **94**, 4609 (1991).
[30](a) Ph. Avouris, J. Phys. Chem. **94**, 2246 (1990); (b) Ph. Avouris, I.-W. Lyo, and F. Bozso, J. Vac. Sci. Technol. B **9**, 424 (1990); (c) Ph. Avouris and F. Bozso, J. Phys. Chem. **94**, 2243 (1990).
[31]F. Bozso and Ph. Avouris, Phys. Rev. B (in press).
[32]L. J. Richter, S. A. Buntin, D. S. King, and R. R. Cavanagh, J. Chem. Phys. **96**, 2324 (1992).
[33]W. Ho, DIET IV, edited by G. Betz and P. Varga (Springer-Verlag, Berlin, 1990), p. 48.
[34]S. K. So and W. Ho, Appl. Phys. A **47**, 213 (1988).
[35]Z. Ying and W. Ho, Phys. Rev. Lett. **60**, 57 (1988).
[36]V. Liberman, G. Haase, and R. M. Osgood, Jr., J. Chem. Phys. (in press).
[37]Y. Chen, J. M. Seo, F. Stepniak, and J. M. Weaver, J. Chem. Phys. **95**, 8442 (1991).
[38]R. D. Dupuis (private communication).